Sparsity optimized high order finite element functions on simplices

S. Beuchler, V. Pillwein, J. Schöberl and S. Zaglmayr

Abstract This article reports several results on sparsity optimized basis functions for hp-FEM on triangular and tetrahedral finite element meshes obtained within the Special Research Program "Numerical and Symbolic Scientific Computing" and within the Doctoral Program "Computational Mathematics" both supported by the Austrian Science Fund FWF under the grants SFB F013 and DK W1214, respectively. We give an overview on the sparsity pattern for mass and stiffness matrix in the spaces L_2, H^1, $H(\mathrm{div})$ and $H(\mathrm{curl})$. The construction relies on a tensor-product based construction with properly weighted Jacobi polynomials.

1 Introduction

Finite element methods (FEM) are among to the most powerful tools for the approximate solution of elliptic boundary value problems of the form: Find $u \in \mathbb{V}$ such that

$$a(u,v) = F(v) \quad \forall v \in \mathbb{V}, \tag{1}$$

where $\mathbb{V}$ is an infinite dimensional Sobolev space of functions on a bounded Lipschitz domain $\Omega \subset \mathbb{R}^d$, $d = 2,3$, $a(\cdot,\cdot) : \mathbb{V} \times \mathbb{V} \mapsto \mathbb{R}$ is an elliptic and bounded bilinear form and $F(\cdot) : \mathbb{V} \mapsto \mathbb{R}$ is a bounded linear functional. Examples for the choice of $a(\cdot,\cdot)$ and $\mathbb{V}$ are

1. the L_2 case, where $\mathbb{V} = L_2(\Omega)$ and $a(u,v) = \int_\Omega uv$,
2. the H^1 case, where $\mathbb{V} = H^1(\Omega)$ and $a(u,v) = \int_\Omega \nabla u \cdot \nabla v + uv$,
3. the $H(\mathrm{div})$ case, where $\mathbb{V} = H(\mathrm{div},\Omega)$ and $a(u,v) = \int_\Omega \nabla \cdot u \, \nabla \cdot v + u \cdot v$,
4. the $H(\mathrm{curl})$ case, where $\mathbb{V} = H(\mathrm{curl},\Omega)$ and $a(u,v) = \int_\Omega \nabla \times u \cdot \nabla \times v + u \cdot v$,

where the space $\mathbb{V}$ coincides with $\{v \in L_2(\Omega) : a(v,v) < \infty\}$. For a general overview of the involved spaces including their finite element approximation we refer to [48].

Research Institute for Symbolic Computation, Johannes Kepler University Linz, 4040 Linz, Austria
e-mail: veronika.pillwein@risc.jku.at (corresponding author)

In all examples, the computation of an approximate solution u_N to u of (1) requires the solution of a linear system of algebraic equations

$$\mathscr{A}\underline{u} = \underline{f} \quad \text{with} \quad \mathscr{A} = [a(\psi_j, \psi_i)]_{i,j=1}^N \tag{2}$$

where $\psi = [\psi_1, \dots, \psi_N]$ is a basis of a finite dimensional subspace $\mathbb{V}_N$ of $\mathbb{V}$, see e.g. [21, 26, 53].
In order to obtain a good approximation u_N to u for a fixed space dimension N of $\mathbb{V}_N$, finite elements with higher polynomial degrees p, e.g. the p and hp-version of the FEM, are preferred if the solution is piecewise smooth, see e.g. [42, 56, 58, 31, 28, 7] and the references therein. The fast solution of (2) with an iterative solution method like the preconditioned conjugate gradient method requires two main ingredients,

- a fast matrix vector multiplication $\mathscr{A}\underline{u}$,
- the choice of a good preconditioner in order to accelerate the iteration process.

Preconditioners based on domain decomposition methods (DD) for hp-FEM are extensively investigated in the literature, see e.g. [33, 8, 51, 39, 40, 38, 2, 41, 5, 12, 44, 18, 46, 13] for the construction of DD-preconditioners and see [10, 49, 4, 27, 29, 30, 11] for extension operators which are required as one ingredient of the DD-preconditioners. The matrix vector multiplication becomes fast if $\mathscr{A}$ is a matrix that has as many non-zero entries as possible, i.e., it is a sparse matrix. Since the global stiffness matrix $\mathscr{A}$ in finite element methods is the result of assembling of local stiffness matrices, it is sufficient to consider the matrices on the element level. In this survey, we will summarize the choice of sparsity optimized basis functions and the results for the above defined bilinear forms on triangular and tetrahedral finite elements. The results and their proofs have been presented in [19, 15, 14, 16], see also [9, 34, 57, 32, 3, 54] for the construction of scalar- and vector-valued high-order finite elements. For fast integration techniques we refer to [42, 36, 47].
For proving the sparsity pattern of the various system matrices we use a symbolic rewriting procedure to evaluate the integrals that determine the matrix entries explicitly. For this rewriting procedure several identities relating several orthogonal polynomials are necessary. Over the past decades algorithms for proving and finding such identities have been developed such as Zeilberger's algorithm [61, 64, 63, 65] or Chyzak's approach [24, 25, 23]. For a general overview on this type of algorithms see, e.g., [52].
The outline of this overview is as follows. Section 2 comprises several results about Jacobi and integrated Jacobi polynomials which are crucial for the sparsity of the system matrices. Some general basics for the definition of tensor product based shape functions on simplicial finite elements are presented in section 3. The sections 4-7 include a summary of the definition of the basis functions and the sparsity results for mass and main term in L_2, H^1, $H(\nabla\cdot)$, and $H(\mathrm{curl})$, respectively. Section 8 gives a brief overview on the algorithm applied for symbolic computation of the matrix entries.

2 Properties of Jacobi polynomials with weight $(1-x)^\alpha$

Sparsity optimization of high-order basis functions on simplices relies on using Jacobi-type polynomials and their basic properties which will be introduced in this section.
For $n \geq 0, \alpha, \beta > -1$ and $x \in [-1,1]$ let

$$P_n^{(\alpha,\beta)}(x) = \frac{(-1)^n}{2^n n!(1-x)^\alpha(1+x)^\beta} \frac{\mathrm{d}^n}{\mathrm{d}x^n}\left((1-x)^{n+\alpha}(1+x)^{n+\beta}\right) \tag{3}$$

be the nth Jacobi polynomial with respect to the weight function $(1-x)^\alpha(1+x)^\beta$. The function $P_n^{(\alpha,\beta)}(x)$ is a polynomial of degree n, i.e. $P_n^{(\alpha,\beta)}(x) \in \mathbb{P}_n((-1,1))$, where $\mathbb{P}_n(I)$ is the space of all polynomials of degree n on the interval I. In the special case $\alpha = \beta = 0$, the functions $P_n^{(0,0)}(x)$ are called Legendre polynomials. Mainly, we will use Jacobi polynomials with $\beta = 0$. For sake of simple notation we therefore omit the second index in (3) and write $p_n^\alpha(x) := P_n^{(\alpha,0)}(x)$.
These polynomials are orthogonal with respect to the weight $(1-x)^\alpha$, i.e. there holds

$$\int_{-1}^{1} (1-x)^\alpha p_j^\alpha(x) p_l^\alpha(x)\,\mathrm{d}x = \rho_j^\alpha \delta_{jl}, \quad \text{where} \quad \rho_j^\alpha = \frac{2^{\alpha+1}}{2j+\alpha+1}. \tag{4}$$

This relation will be heavily used in computing the entries of the different mass and stiffness matrices. Moreover for $n \geq 1$, let

$$\hat{p}_n^\alpha(x) = \int_{-1}^{x} p_{n-1}^\alpha(y)\,\mathrm{d}y, \quad \text{with} \quad \hat{p}_0^\alpha(x) = 1, \tag{5}$$

be the nth integrated Jacobi polynomial. Obviously, $\hat{p}_n^\alpha(-1) = 0$ for $n \geq 1$. Integrated Legendre polynomials, by the orthogonality relation (4), vanish at both endpoints of the interval. Summarizing, one obtains

$$\hat{p}_n^\alpha(-1) = 0, \quad \hat{p}_n^0(1) = 0 \quad \text{for } n \geq 2. \tag{6}$$

Factoring out these roots, integrated Jacobi polynomials (5) can be expressed in terms of Jacobi polynomials (3) with modified weights, i.e.,

$$\hat{p}_n^\alpha(x) = \frac{1+x}{n} P_{n-1}^{(\alpha-1,1)}(x), \qquad n \geq 1, \tag{7}$$

$$\hat{p}_n^0(x) = \frac{1-x^2}{2n-2} P_{n-2}^{(1,1)}(x), \qquad n \geq 2. \tag{8}$$

There are several further identities relating Jacobi polynomials $p_n^\alpha(x)$ and integrated Jacobi polynomials (5) that have been proven in [19], [14] and [15]. These include three term recurrences for fast evaluation as well as identities necessary for proving the sparsity pattern of the mass and stiffness matrices below. We give a summary

of all necessary identities in section 8. For more details on Jacobi polynomials we refer the interested reader to the books of Abramowitz and Stegun [1], Szegö [59], and Tricomi [60].

3 Preliminary definitions

We assume a conforming affine simplicial mesh. Although the basis functions are defined on arbitrary simplices, the analysis of the basis functions can be performed only on the reference elements $\hat{T}$ as defined in Figure 1. The sparsity result on affine meshes then follows by the mapping principle. An arbitrary simplex can be mapped by an affine transformation to these reference elements. We mention that affine transformations guarantee that polynomials are mapped to polynomials of the same degree. The basis functions will be defined by means of barycentric coordinates λ_i that are functions depending on x, y (and z). For our reference triangle they are given as

$$\lambda_1(x,y) = \frac{1-2x-y}{4}, \quad \lambda_2(x,y) = \frac{1+2x-y}{4}, \quad \text{and} \quad \lambda_3(x,y) = \frac{1+y}{2},$$

and for the reference tetrahedron they are defined as

$$\lambda_{1/2}(x,y,z) = \frac{1\mp 4x-2y-z}{8}, \quad \lambda_3(x,y,z) = \frac{1+2y-z}{4}, \quad \text{and} \quad \lambda_4(x,y,z) = \frac{1+z}{2}.$$

We mention that the barycentric coordinates add up to 1.

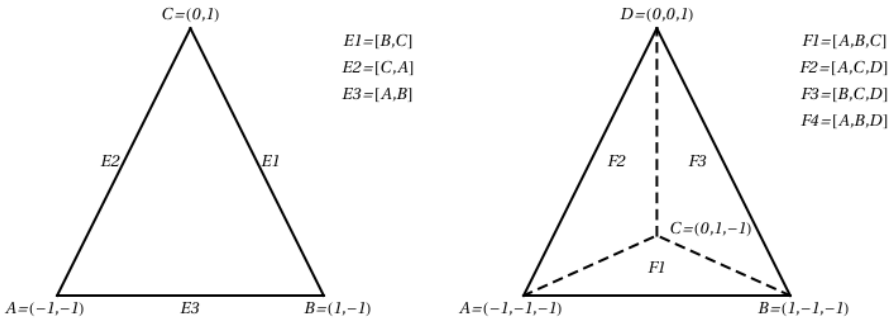

Fig. 1 Notation of the vertices and edges/faces on the reference element $\hat{T}$ for 2d and 3d.

By viewing the triangle (tetrahedron) as a collapsed quadrilateral (hexahedron) as suggested by Dubiner [34] and Karniadakis, Sherwin [42], we can construct a tensorial-type basis also for simplices. For this purpose, we need the Duffy transformation that maps the tensorial element to the simplicial element.

In 2 dimensions the Duffy transformation $\mathscr{D}$ mapping the unit square to the reference triangle is defined as

$$\begin{array}{rl} \mathscr{D}: \hat{Q} = [-1,1]^2 \to & \hat{T} \\ (\xi,\eta) & \to (x,y) \end{array} \quad \text{with} \quad \begin{array}{l} x = \frac{\xi}{2}(1-\eta), \\ y = \eta. \end{array} \tag{9}$$

Using the inverse of the Duffy transformation, we can parameterize the triangle $\hat{\triangle}$ by

$$\xi = \frac{2x}{1-y} = \frac{\lambda_2(x,y)-\lambda_1(x,y)}{\lambda_2(x,y)+\lambda_1(x,y)}, \quad \text{and} \quad \eta = y = 2\lambda_3(x,y)-1.$$

Besides the Duffy transformation, polynomial basis functions which vanish on some or all edges of the triangle are required. Therefore, we introduce several auxiliary bubble functions, which are important for the definition of our basis functions. More precisely, the authors introduce the edge based function

$$g_i^E(x,y) := \hat{p}_i^0\left(\tfrac{\lambda_{e_2}-\lambda_{e_1}}{\lambda_{e_1}+\lambda_{e_2}}\right)(\lambda_{e_1}+\lambda_{e_2})^i \tag{10}$$

on the edge $E = [e_1, e_2]$, running from vertex V_{e_1} to V_{e_2} and the bubbles

$$g_i(x,y) := \hat{p}_i^0\left(\tfrac{\lambda_2-\lambda_1}{\lambda_1+\lambda_2}\right)(\lambda_1+\lambda_2)^i \quad \text{and} \quad h_{ij}(x,y) := \hat{p}_j^{2i-1}(2\lambda_3-1), \tag{11}$$

where the barycentric coordinates depend on x and y. Note that the functions in (10) and (11) are polynomial functions of degrees i, i and j, respectively. Using (6), one observes that the functions g_i^E as defined in (10) vanish at the endpoints of the edge E. In the same way, the functions $g_i(x,y)$ vanish at the edges $E2 = [1,3]$ and $E3 = [2,3]$, whereas h_{ij} vanishes at the edge $E1 = [1,2]$.
In 3 dimensions the Duffy transformation mapping the unit cube to the reference tetrahedron is defined as

$$\begin{array}{rl} \mathscr{D}: \hat{Q} = [-1,1]^3 \to & \hat{T} \\ (\xi,\eta,\zeta) & \to (x,y,z) \end{array} \quad \text{with} \quad \begin{array}{l} x = \frac{\xi}{4}(1-\eta)(1-\zeta), \\ y = \frac{\eta}{2}(1-\zeta), \\ z = \zeta. \end{array}$$

Using the inverse of the Duffy transformation we can parameterize the triangle $\hat{\triangle}$ by

$$\begin{aligned} \xi &= \frac{4x}{1-2y-z} = \frac{\lambda_2(x,y,z)-\lambda_1(x,y,z)}{\lambda_2(x,y,z)+\lambda_1(x,y,z)}, \\ \eta &= \frac{2y}{1-z} = \frac{\lambda_3(x,y,z)-\lambda_2(x,y,z)-\lambda_1(x,y,z)}{\lambda_3(x,y,z)+\lambda_2(x,y,z)+\lambda_1(x,y,z)}, \\ \zeta &= z = 2\lambda_4(x,y,z)-1. \end{aligned}$$

Here, the edge-based functions

$$u_i^E(x,y,z) := \hat{p}_i^0\left(\tfrac{\lambda_{e_2}-\lambda_{e_1}}{\lambda_{e_1}+\lambda_{e_2}}\right)(\lambda_{e_1}+\lambda_{e_2})^i \tag{12}$$

are introduced on the edge $E=[e_1,e_2]$, running from vertex V_{e_1} to V_{e_2}. The face based functions

$$u_i^F := \hat{p}_i^0\left(\frac{\lambda_{f_2}-\lambda_{f_1}}{\lambda_{f_2}+\lambda_{f_1}}\right)(\lambda_{f_2}+\lambda_{f_1})^i, \qquad v_{ij}^F := \hat{p}_j^{2i-1}(\lambda_{f_3}-\lambda_{f_2}-\lambda_{f_1}) \tag{13}$$

are defined on the face $F=[f_1,f_2,f_3]$ characterized by the vertices V_{f_1},V_{f_2} and V_{f_3}. The functions

$$\begin{aligned} u_i(x,y,z) &:= \hat{p}_i^0\left(\frac{\lambda_2-\lambda_1}{\lambda_2+\lambda_1}\right)(\lambda_2+\lambda_1)^i, \\ v_{ij}(x,y,z) &:= \hat{p}_j^{2i-1}\left(\frac{2\lambda_3-(1-\lambda_4)}{1-\lambda_4}\right)(1-\lambda_4)^j, \\ \text{and}\quad w_{ijk}(x,y,z) &:= \hat{p}_k^{2i+2j-2}(2\lambda_4-1) \end{aligned} \tag{14}$$

will be central in the definition of the interior bubble functions. Again, the barycentric coordinates depend on x, y and z. For vector valued problems, the lowest-order Nédélec function [50] corresponding to the edge $E=[e_1,e_2]$ and the lowest order Raviart-Thomas function, [50, 20], corresponding to $F=[f_1,f_2,f_3]$, characterized by the vertices V_{f_1},V_{f_2} and V_{f_3} are defined by

$$\varphi_{1,E} := \nabla\lambda_{e_1}\lambda_{e_2}-\lambda_{e_1}\nabla\lambda_{e_2} \quad \text{and} \tag{15}$$

$$\psi_0^F \;=\; \psi_0^{[f_1,f_2,f_3]} := \lambda_{f_1}\nabla\lambda_{f_2}\times\nabla\lambda_{f_3}+\lambda_{f_2}\nabla\lambda_{f_3}\times\nabla\lambda_{f_1}+\lambda_{f_3}\nabla\lambda_{f_1}\times\nabla\lambda_{f_2}, \tag{16}$$

respectively.
The functions (10)-(14) and the choice of the weights for the Jacobi polynomials are pivotal for obtaining the sparsity results in mass and stiffness matrices.

4 The L_2 orthogonal basis functions of Dubiner

These basis functions have been introduced by [34], see also [42]. Another possible construction principle is based on Appell polynomials, [6, 22, 35].
Let $\triangle_s$ be a triangle with its baryzentrical coordinates $\lambda_m(x,y)$, $m=1,2,3$. Instead of (11), we introduce the auxiliary functions

$$\tilde{g}_i(x,y) := p_i^0\left(\tfrac{\lambda_2-\lambda_1}{\lambda_1+\lambda_2}\right)(\lambda_1+\lambda_2)^i \quad \text{and} \quad \tilde{h}_{ij}(x,y) := p_j^{2i+1}(2\lambda_3-1),$$

and define the L_2 orthogonal functions

$$\psi_{ij}(x,y) = \tilde{g}_i(x,y)\tilde{h}_{ij}(x,y), \quad 0\le i,j,\ i+j\le p.$$

We prove this orthogonality for the reference triangle given in Figure 1. The computations are straight forward: after using the Duffy transformation the integrals

can be evaluated by a mere application of the orthogonality relation (4) for Jacobi polynomials:

$$\begin{aligned}
&\int_{\hat{T}} p_i^0\left(\frac{2x}{1-y}\right) p_k^0\left(\frac{2x}{1-y}\right)\left(\frac{1-y}{2}\right)^{i+k} p_j^{2i+1}(y)p_l^{2k+1}(y)\,\mathrm{d}(x,y)\\
=&\int_{-1}^1 p_i^0(\xi)p_k^0(\xi)\,\mathrm{d}\xi\int_{-1}^1\left(\frac{1-\eta}{2}\right)^{i+k+1} p_j^{2i+1}(\eta)p_l^{2k+1}(\eta)\,\mathrm{d}\eta\\
=&\frac{2}{2i+1}\delta_{ik}\int_{-1}^1\left(\frac{1-\eta}{2}\right)^{2i+1} p_j^{2i+1}(\eta)p_l^{2i+1}(\eta)\,\mathrm{d}\eta\\
=&\frac{2\delta_{ik}\delta_{jl}}{(2i+1)(i+j+1)}.
\end{aligned}$$

Now, let $\triangle_s$ be a tetrahedron with its baryzentrical coordinates $\lambda_m(x,y)$, $m=1,2,3,4$. With the auxiliary functions

$$\begin{aligned}
\tilde{u}_i(x,y,z) &:= p_i^0\left(\frac{\lambda_2-\lambda_1}{\lambda_2+\lambda_1}\right)(\lambda_2+\lambda_1)^i,\\
\tilde{v}_{ij}(x,y,z) &:= p_j^{2i+1}\left(\frac{\lambda_3-\lambda_2-\lambda_1}{\lambda_3+\lambda_2+\lambda_1}\right)(\lambda_3+\lambda_2+\lambda_1)^j,\\
\text{and}\quad \tilde{w}_{ijk}(x,y,z) &:= p_k^{2i+2j+2}(\lambda_4-\lambda_1-\lambda_2-\lambda_3)
\end{aligned}$$

the basis functions read as

$$\psi_{ijk}(x,y,z) := \tilde{u}_i(x,y,z)\tilde{v}_{ij}(x,y,z)\tilde{w}_{ijk}(x,y,z),\quad i+j+k\le p, i,j,k\ge 0.$$

The evaluation of the L_2-inner product is completely analogous to the triangular case. For the reference tetrahedron as defined in Figure 1, the final result is

$$\int_{\hat{T}}\psi_{ijk}(x,y,z)\psi_{lmn}(x,y,z)\,\mathrm{d}(x,y,z) = \frac{4\delta_{il}\delta_{jm}\delta_{kn}}{(2i+1)(i+j+1)(2i+2j+2k+3)}.$$

Also the sparsity results for the basis functions for H^1, $H(\mathrm{div})$ and $H(\mathrm{curl})$ are proved by evaluation that proceeds by rewriting until the orthogonality relation (4) for Jacobi polynomials can be exploited. These computations, however, become much more evolved as indicated in the sections below and ultimately this task is handed over to an algorithm, see section 8.

5 Sparsity optimized H^1-conforming basis functions

The construction of the basis functions in this section follows [14, 15, 19]. Throughout we assume a uniform polynomial degree p.

In order to obtain H^1-conforming functions, the global basis functions have to be globally continuous. In 2D, the functions are split into 3 different groups, the vertex based functions, the edge bubble functions and the interior bubbles. In order to guarantee a simple continuous extension to the neighboring element, the interior bubbles are defined to vanish at all element edges, the edge bubbles vanish on two of the three edges whereas the vertex functions are chosen as the usual hat functions. In 3D, there additionally exist face bubble functions.

5.1 Sparse H^1-conforming basis functions on the triangle

Using the integrated Jacobi polynomials (5), we define the shape functions on the affine triangle $\triangle_s$ with baryzentrical coordinates $\lambda_m(x,y)$, $m=1,2,3$.

- The vertex functions are chosen as the usual linear hat functions

$$\psi_{V,m}(x,y) := \lambda_m(x,y), \quad m=1,2,3.$$

  Let $\Psi_V^2 := [\psi_{V,1}, \psi_{V,2}, \psi_{V,3}]$ be the basis of the vertex functions.
- For each edge $E=[e_1,e_2]$, running from vertex V_{e_1} to V_{e_2}, we define

$$\psi_{[e_1,e_2],i}(x,y) = g_i^E(x,y)$$

  with the integrated Legendre type functions (10). By $\Psi_{[e_1,e_2]} = \left[\psi_{[e_1,e_2],i}\right]_{i=2}^{p}$, we denote the basis of the edge bubble functions on the edge $[e_1,e_2]$. $\Psi_E^2 = \left[\Psi_{[1,2]}, \Psi_{[2,3]}, \Psi_{[3,1]}\right]$ is the basis of all edge bubble functions.
- The interior bubbles are defined as

$$\psi_{ij}(x,y) := g_i(x,y)h_{ij}(x,y), \quad i+j \le p, i \ge 2, j \ge 1, \tag{17}$$

  where the auxiliary bubble functions g_i and h_{ij} are given in (11). Moreover, $\Psi_I^2 = [\psi_{ij}]_{i\ge 2, j\ge 1}^{i+j\le p}$ denotes the basis of all interior bubbles.

Finally, let $\Psi_{\nabla,2} = \left[\Psi_V^2, \Psi_E^2, \Psi_I^2\right]$ be the set of all shape functions on $\triangle_s$.
The interior block of the mass and stiffness matrix on the triangle $\triangle_s$ are denoted by

$$M_{II,s,\nabla_2} = \int_{\triangle_s} [\Psi_I^2]^\top [\Psi_I^2] := \left[\mu_{ij;kl}^{s,2}\right]_{i,k=2;j,l=1}^{i+j\le p;k+l\le p}, \quad \text{and} \tag{18}$$

$$K_{II,s,\nabla_2} = \int_{\triangle_s} [\nabla\Psi_I^2]^\top \cdot [\nabla\Psi_I^2] := \left[a_{ij;kl}^{s,2}\right]_{i,k=2;j,l=1}^{i+j\le p;k+l\le p}, \tag{19}$$

respectively.

Theorem 5.1 *Let M_{II,s,∇_2} be defined via* (18)*, then the matrix has $\mathcal{O}(p^2)$ nonzero matrix entries. More precisely, $\mu_{ij;kl}^{s,2} = 0$ if $|i-k| \notin \{0,2\}$ or $|i-k+j-l| > 4$.*

Let K_{II,s,∇_2} be defined via (19)*, then the matrix has $\mathcal{O}(p^2)$ nonzero matrix entries. More precisely, $a^{s,2}_{ij;kl} = 0$ if $|i-k| > 2$ or $|i-k+j-l| > 2$.*

Proof. This sparsity result is proven by explicit evaluation of the matrix entries using the algorithm described in section 8, see also [14, 15]. However, we will give the interested reader a short impression of the proofs. After the affine linear mapping of the element $\triangle_s$ to the reference element $\hat{\triangle}$ it suffices to prove the results there. We start with sketching the result for the mass matrix.
On the reference element $\hat{T}$, we have

$$\hat{\mu}^{(2)}_{ij;kl} = \int_{\hat{T}} \hat{p}^0_i \left(\frac{2x}{1-y}\right) \left(\frac{1-y}{2}\right)^i \hat{p}^{2i-1}_j(y) \hat{p}^0_k \left(\frac{2x}{1-y}\right) \left(\frac{1-y}{2}\right)^k \hat{p}^{2k-1}_l(y) \,\mathrm{d}(x,y)$$

by (11) and (17). With the substitution $\xi = \frac{2x}{1-y}$ and $\eta = y$, cf. (9), the integral simplifies to

$$\hat{\mu}^{(2)}_{ij;kl} = \int_{-1}^1 \hat{p}^0_i(\xi) \hat{p}^0_k(\xi) \,\mathrm{d}\xi \int_{-1}^1 \left(\frac{1-\eta}{2}\right)^{i+k+1} \hat{p}^{2i-1}_j(\eta) \hat{p}^{2k-1}_l(\eta) \,\mathrm{d}\eta.$$

Using (35) for $\alpha = 0$, the integrated Legendre polynomials can be expressed as the sum of two Legendre polynomials. The orthogonality relation (4) implies that the first integral is zero if $|i-k| \notin \{0,2\}$.
For $i = k$, we obtain

$$\hat{\mu}^{(2)}_{ij;il} = c_i \int_{-1}^1 \left(\frac{1-\eta}{2}\right)^{2i+1} \hat{p}^{2i-1}_j(\eta) \hat{p}^{2i-1}_l(\eta) \,\mathrm{d}\eta$$

with some constants c_i. Now, relation (36) is applied for $\hat{p}^{2i-1}_j(\eta)$ and $\hat{p}^{2i-1}_l(\eta)$. This gives

$$\hat{\mu}^{(2)}_{ij;il} = c_{i,j,l} \int_{-1}^1 \left(\frac{1-\eta}{2}\right)^{2i+1} (p^{2i-1}_j(\eta) + p^{2i-1}_{j-1}(\eta))(p^{2i-1}_l(\eta) + p^{2i-1}_{l-1}(\eta)) \,\mathrm{d}\eta.$$

By the orthogonality relation (4), the term $(p^{2i-1}_j(\eta) + p^{2i-1}_{j-1}(\eta))$ is orthogonal to all polynomials of maximal degree $j-2$ with respect to the weight $\left(\frac{1-\eta}{2}\right)^{2i-1}$, e.g., is orthogonal to $\left(\frac{1-\eta}{2}\right)^2 (p^{2i-1}_l(\eta) + p^{2i-1}_{l-1}(\eta)) \in \mathbb{P}_l$. Therefore, $\hat{\mu}^{(2)}_{ij;il} = 0$ for $j-l > 4$. By symmetry, we obtain $\hat{\mu}^{(2)}_{ij;il} = 0$ for $|j-l| > 4$. For $k = i-2$, one obtains

$$\hat{\mu}^{(2)}_{ij;i-2l} = c_i \int_{-1}^1 \left(\frac{1-\eta}{2}\right)^{2i-1} \hat{p}^{2i-1}_j(\eta) \hat{p}^{2i-5}_l(\eta) \,\mathrm{d}\eta.$$

Again, by (36) and (4), the result $\hat{\mu}_{ij;i-2l} = 0$ for $|j+2-l| > 4$ follows.
For the stiffness matrix, the proof is similar. Starting point is the computation of the gradient on the reference element, which is given by

$$\nabla\psi_{ij} = \begin{bmatrix} p_{i-1}^0\left(\frac{2x}{1-y}\right)\left(\frac{1-y}{2}\right)^{i-1}\hat{p}_j^{2i-1}(y) \\ \frac{1}{2}p_{i-2}^0\left(\frac{2x}{1-y}\right)\left(\frac{1-y}{2}\right)^{i-1}\hat{p}_j^{2i-1}(y) + \hat{p}_i^0\left(\frac{2x}{1-y}\right)\left(\frac{1-y}{2}\right)^{i} p_{j-1}^{2i-1}(y) \end{bmatrix}.$$

With this closed form representation at hand the computations follow the same pattern as outlined for the mass matrix.

Remark 5.2 *The family of basis functions defined by the auxiliary functions*

$$g_i(x,y) := \hat{p}_i^0\left(\frac{\lambda_2-\lambda_1}{\lambda_1+\lambda_2}\right)(\lambda_1+\lambda_2)^i \quad \textit{and} \quad h_{ij}(x,y) := \hat{p}_j^{2i-a}(2\lambda_3-1), \tag{20}$$

for $0 \le a \le 4$ *have been considered in [15]. For* $a = 1$*, the functions coincide with the functions given in* (11)*. The sparsity optimal basis for* H^1 *for both mass and stiffness matrix is given by the choice* $a = 0$ *which also yields the best condition numbers for the system matrix.*

The nonzero pattern obtained by Theorem 5.1 is displayed in Figure 2 for the interior basis functions (17) obtained by (20) with $a = 0$ and $a = 1$. The best sparsity results are obtained for $a = 0$ with a maximum of 9 nonzero entries per row for the element stiffness matrix on the reference element $\hat{\triangle}$. Because of this change of the weights in (20), the bandwidths of the nonzero blocks become larger for $a = 1$.
This nonzero pattern has a stencil like structure which makes it simpler to solve systems with linear combinations of M_{II,s,∇_2} and K_{II,s,∇_2} using sparse direct solvers as the method of nested dissection, [37], embedded in a DD-preconditioner. This is an important tool if static condensation is used in order to solve the system (2). We refer the interested reader for a more detailed discussion to [19].
Besides the sparsity, also the condition numbers of the local matrices are important. Figure 3 displays the diagonally preconditioned condition numbers of the stiffness matrix $\hat{K}_{II,\nabla_2}$ (19) on the reference element $\hat{T}$ for several polynomial degrees. Numerically the condition number grows at least as $\mathcal{O}(p^2)$ for the functions with $a = 0$. This is the best possible choice for interior bubbles in two space dimensions.

5.2 Sparse H^1-conforming basis functions on the tetrahedron

The construction principle follows [14].

- The vertex functions are defined as the usual hat functions, i.e.

$$\psi_{V,m}(x,y,z) = \lambda_m(x,y,z), \quad m = 1,2,3,4.$$

  Let $\Psi_V^3 = [\psi_{V,m}]_{m=1}^4$ denote the basis of the hat functions.
- With (12), the edge bubbles are defined as

$$\psi_i^{[e_1,e_2]}(x,y) := u_i^E(x,y), \quad \text{for } 2 \le i \le p$$

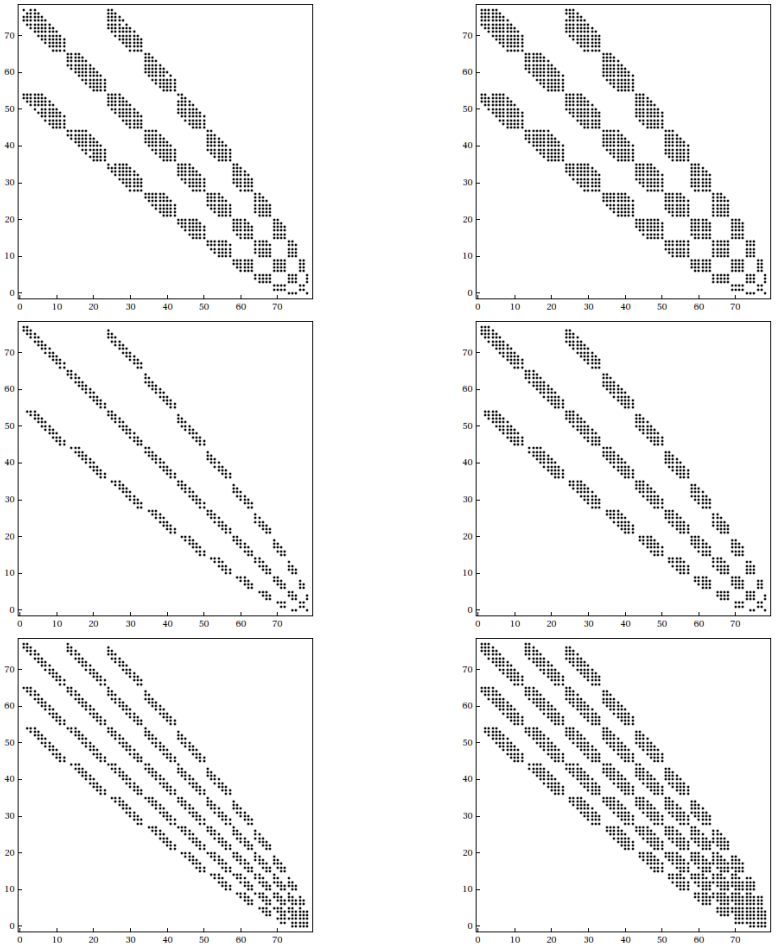

Fig. 2 Nonzero pattern for $p = 14$: mass matrix M_{II,s,∇_2} (above), stiffness matrix $\hat{K}_{II,\nabla_2}$ on $\hat{T}$ (middle), stiffness matrix K_{II,s,∇_2} on general element (below) for the interior bubbles based on the functions (20) with $a = 0$ (left) and $a = 1$ (right).

for an edge $E = [e_1, e_2]$, running from vertex V_{e_1} to V_{e_2}. We denote the basis of all edge bubble functions by

$$\Psi_E^3 = \left[\left[\psi_i^{[1,2]} \right]_{i=2}^p, \left[\psi_i^{[2,3]} \right]_{i=2}^p, \left[\psi_i^{[3,1]} \right]_{i=2}^p, \left[\psi_i^{[1,4]} \right]_{i=2}^p, \left[\psi_i^{[2,4]} \right]_{i=2}^p, \left[\psi_i^{[3,4]} \right]_{i=2}^p \right].$$

- For each face $F = [f_1, f_2, f_3]$, characterized by the vertices V_{f_1}, V_{f_2} and V_{f_3}, the face bubbles are defined as

$$\psi_{j,k}^f(x,y,z) := u_i^F(x,y,z)\, v_{ij}^F(x,y,z), \quad i \geq 2, j \geq 1, i+j \leq p$$

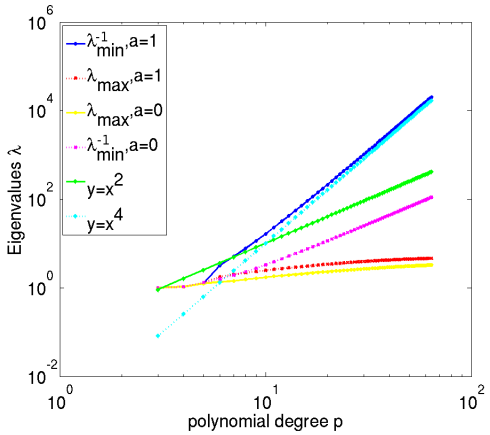

Fig. 3 Maximal and reciprocals of the minimal eigenvalues for the stiffness matrix $\hat{K}_{II,\nabla_2}$ (19) on the reference element $\hat{T}$ for the basis functions based on (20) with $a=0$ and $a=1$.

using the functions (13). We denote the basis of all face bubble functions by

$$\Psi_F^3 := \left[\left[\psi_{i,j}^{[1,2,3]} \right]_{i=2,j=1}^{i+j=p} \left[\psi_{i,j}^{[2,3,4]} \right]_{i=2,j=1}^{i+j=p}, \left[\psi_{i,j}^{[3,4,1]} \right]_{i=2,j=1}^{i+j=p}, \left[\psi_{i,j}^{[4,1,2]} \right]_{i=2,j=1}^{i+j=p} \right].$$

- With the functions (14), the interior bubbles read as

$$\psi_{ijk}(x,y,z) := u_i(x,y,z) v_{ij}(x,y,z) w_{ijk}(x,y,z), \quad i+j+k \le p, i \ge 2, j,k \ge 1.$$

Moreover, $\Psi_I^3 = \left[\psi_{ijk} \right]_{i\ge 2, j\ge 1, k\ge 1}^{i+j+k\le p}$ denotes the basis of the interior bubbles.

Let $\Psi_{\nabla,3} = \left[\Psi_V^3, \Psi_E^3, \Psi_F^3, \Psi_I^3 \right]$ be the basis of all shape functions.
The interior block of the mass and stiffness matrix on the triangle $\triangle_s$ are denoted by

$$M_{II,s,\nabla_3} = \int_{\triangle_s} [\Psi_I^3]^\top [\Psi_I^3] := \left[\mu_{ijk;lmn}^{s,3} \right]_{i,l=2;j,m,l,n=1}^{i+j+k\le p; l+m+n\le p} \quad \text{and} \tag{21}$$

$$K_{II,s,\nabla_3} = \int_{\triangle_s} [\nabla \Psi_I^3]^\top \cdot [\nabla \Psi_I^3] := \left[a_{ijk;lmn}^{s,3} \right]_{i,l=2;j,k,m,n=1}^{i+j+k\le p; l+m+n\le p}, \tag{22}$$

respectively.

Theorem 5.3 *The inner block of the mass matrix M_{II,s,∇_3} has in total $\mathcal{O}(p^3)$ nonzero matrix entries. More precisely, $\mu_{ijk;mln} = 0$ if $|i-l| > 2$, $|i-l+j-m| > 4$ or $|i-l+j-m+k-n| > 6$.*
The inner block of the stiffness matrix K_{II,s,∇_3} has in total $\mathcal{O}(p^3)$ nonzero matrix entries. More precisely, $\mu_{ijk;mln} = 0$ if $|i-l| > 2$, $|i-l+j-m| > 3$ or $|i-l+j-m+k-n| > 4$.

Proof. Evaluation of the matrix entries using the algorithm described in section 8, see also [14, 15].

Remark 5.4 *In [15], the auxiliary functions are defined in the more general form*

$$\begin{aligned} u_i(x,y,z) &:= \hat{p}_i^0 \left(\frac{\lambda_2-\lambda_1}{\lambda_2+\lambda_1}\right)(\lambda_2+\lambda_1)^i, \\ v_{ij}(x,y,z) &:= \hat{p}_j^{2i-a} \left(\frac{2\lambda_3-(1-\lambda_4)}{1-\lambda_4}\right)(1-\lambda_4)^j, \\ \text{and} \quad w_{ijk}(x,y,z) &:= \hat{p}_k^{2i+2j-b}(2\lambda_4-1), \end{aligned} \tag{23}$$

where the integers a and b satisfy $0 \le a \le 4$, $a \le b \le 6$. *The interior bubbles coincide with the functions given in [57], see also [42], if* $a = b = 0$. *To make this equivalence obvious use the identities* (7) *and* (8). *This choice corresponds to the sparsity optimal case for* H^1 *for both mass and stiffness matrix. In this case the results of Theorem 5.3 reduce to* $|i-l| > 2$, $|i-l+j-m| > 3$ *or* $|i-l+j-m+k-n| > 4$ *for the mass matrix and* $|i-l| > 2$, $|i-l+j-m| > 3$ *or* $|i-l+j-m+k-n| > 2$ *for the stiffness matrix. The auxiliary polynomials used in this paper correspond to setting* $a = 1$ *and* $b = 2$.

Again a stencil like structure for mass and stiffness matrix is obtained. However, the elimination of the interior bubbles by static condensation with nested dissection is much more expensive in the 3D case than in the 2D case. The computational complexity is now $\mathcal{O}(p^6)$ flops in comparison to $\mathcal{O}(p^3)$ flops in the two-dimensional case.

Besides the sparsity, also the condition numbers of the local matrices are important. Figure 4 displays the condition numbers of the stiffness matrix $\hat{K}_{II,\nabla_3}$ (22) on the reference element $\hat{T}$ for several polynomial degrees and several choices of auxiliary functions (14) and (23). Numerically, the condition number grows as least with $\mathcal{O}(p^4)$.

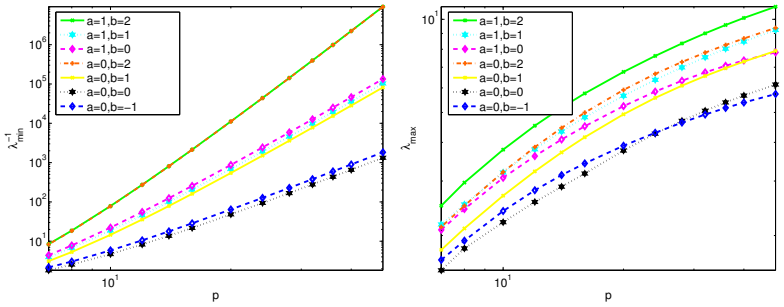

Fig. 4 Maximal (right) and minimal (left) eigenvalues for the diagonally preconditioned stiffness matrix $\hat{K}_{II,\nabla_3}$ (22) on the reference element $\hat{T}$ for different values of a and b in (23).

6 Sparsity optimization of $H(\mathrm{div})$-conforming basis functions

The following construction of $H(\mathrm{div})$-conforming finite elements applies the ideas on sparsity optimization on simplices of [19, 14, 15] to the general construction principles of $H(\mathrm{div})$-conforming high-order fe bases developed in [62] and [55]. A detailed description of both the 2 and 3 dimensional case can be found in [16]. In the sequel, we only report the results for tetrahedra.
Let Δ_s denote an arbitrary non-degenerated simplex $\Delta_s \subset \mathbb{R}^3$, its set of four vertices by $\mathscr{V} = \{V_1, V_2, V_3, V_4\}$, $V_i \in \mathbb{R}^3$, and $\lambda_1, \lambda_2, \lambda_3, \lambda_4 \in P^1(\Delta_s)$ its barycentric coordinates. Global $H(\mathrm{div})$ conformity requires normal continuity over element interfaces, which can be easily achieved by using a face-interior-based high-order finite element basis. The general construction follows [62, 55]: The set of face-based shape functions consists of low-order Raviart-Thomas shape functions and divergence-free shape functions. The set of interior based shape functions are split into a set of divergence-free fields (rotations) and a set of non-divergence-free completion functions. Using the appropriately weighted Jacobi-type polynomials of Section 3 the $H(\mathrm{div})$-conforming shape functions on the tetrahedron are defined as follows.

- For each face $F = [f_1, f_2, f_3]$, characterized by the vertices V_{f_1}, V_{f_2} and V_{f_3} we construct the face based basis functions as follows. First, we choose the classical Raviart-Thomas function of order zero ψ_0^F (16) and add the divergence-free higher-order face based shape functions

$$\begin{aligned} \psi_{1j}^F &:= \nabla \times \left(\varphi_1^{[f_1,f_2]} v_{1j}^F \right), && 1 \le j \le p, \\ \psi_{ij}^F &:= \nabla \times \left(\nabla u_i^F v_{ij}^F \right) = -\nabla u_i^F \times \nabla v_{ij}^F, && 2 \le i; 1 \le j; i+j \le p+1 \end{aligned} \tag{24}$$

  where we use the face-based Jacobi-type polynomials (13) and the lowest-order Nédélec function (15) corresponding to the edge $[f_1, f_2]$. Let

$$[\Psi_0] := \left[\psi_0^{F_1}, \psi_0^{F_2}, \psi_0^{F_3}, \psi_0^{F_4} \right] \tag{25}$$

  denote the row vector of low-order shape functions,

$$[\Psi^F] := \left[\left[\psi_{1j}^F \right]_{j=1}^{p}, \left[\psi_{ij}^F \right]_{i=2,j=1}^{i+j \le p+1} \right]$$

  denote the row vector of the faced-based high-order shape functions of one fixed face F, and

$$[\Psi_F^\cdot] := \left[[\Psi^{F1}] \; [\Psi^{F2}] \; [\Psi^{F3}] \; [\Psi^{F4}] \right] \tag{26}$$

  be the row vector of all face-based high-order shape functions.
- The cell-based basis functions are constructed in two types. First we define the divergence-free shape functions by the rotations

$$\begin{aligned}
\psi^{(a)}_{1jk}(x,y,z) &:= \nabla \times \big(\varphi^{[1,2]}_1(x,y,z)\, v_{2j}(x,y,z)\, w_{2jk}(x,y,z)\big),\\
&\qquad j,k \geq 1;\ j+k \leq p,\\
\psi^{(b)}_{ijk}(x,y,z) &:= \nabla \times \big(\nabla u_i(x,y,z)\, v_{ij}(x,y,z)\, w_{ijk}(x,y,z)\big),\\
&\qquad i \geq 2;\ j,k \geq 1;\ i+j+k \leq p+2,\\
\psi^{(c)}_{ijk}(x,y,z) &:= \nabla \times \big(\nabla(u_i(x,y,z)\ v_{ij}(x,y,z))\ w_{ijk}(x,y,z)\big),\\
&\qquad i \geq 2;\ j,k \geq 1;\ i+j+k \leq p+2,
\end{aligned}$$

and complete the basis with the non-divergence free cell-based shape functions

$$\begin{aligned}
\widetilde{\psi}^{(a)}_{10k}(x,y,z) &:= \psi^{[1,2,3]}_0(x,y,z)\, w_{21k}(x,y,z),\\
&\qquad 1 \leq k \leq p-1,\\
\widetilde{\psi}^{(b)}_{1jk}(x,y,z) &:= \varphi^{[1,2]}_0(x,y,z) \times \nabla w_{2jk}(x,y,z)\, v_{2j}(x,y,z),\\
&\qquad j,k \geq 1;\ j+k \leq p,\\
\widetilde{\psi}^{(c)}_{ijk}(x,y,z) &:= w_{ijk}(x,y,z)\, \nabla u_i(x,y,z) \times \nabla v_{ij}(x,y,z),\\
&\qquad i \geq 2;\ j,k \geq 1;\ i+j+k \leq p+2,
\end{aligned}$$

where $\psi^{[1,2,3]}_0(x,y,z)$ denotes the Raviart-Thomas function (16) associated to the bottom face $[1,2,3]$ and $\varphi^{[1,2]}_0$ is the Nédélec function (15) associated to the edge $[1,2]$. The auxiliary functions u_i, v_{ij} and w_{ijk} have been defined in (14).
Finally, we denote the row vectors of the corresponding basis functions as

- $[\Psi_a] = \Big[\psi^{(a)}_{1jk}(x,y,z)\Big]^{j+k\leq p}_{j,k,\geq 1}$,
- $[\Psi_b] = \Big[\psi^{(b)}_{ijk}(x,y,z)\Big]^{i+j+k\leq p+2}_{i\geq 2,j,k,\geq 1}$,
- $[\Psi_c] = \Big[\psi^{(c)}_{ijk}(x,y,z)\Big]^{i+j+k\leq p+2}_{i\geq 2,j,k,\geq 1}$, for the divergence-free parts, and
- $[\widetilde{\Psi}_a] = \Big[\widetilde{\psi}^{(a)}_{10k}(x,y,z)\Big]^{p-1}_{k=1}$,
- $[\widetilde{\Psi}_b] = \Big[\widetilde{\psi}^{(b)}_{1jk}(x,y,z)\Big]^{j+k\leq p}_{j,k,\geq 1}$, and
- $[\widetilde{\Psi}_c] = \Big[\widetilde{\psi}^{(c)}_{ijk}(x,y,z)\Big]^{i+j+k\leq p+2}_{i\geq 2,j,k,\geq 1}$ for the non divergence-free polynomials.

The set of the interior shape functions is denoted by

$$[\Psi_I] := \big[\,[\Psi_1]\ [\Psi_2]\,\big] \ \text{ with } \quad [\Psi_1] := \big[\,[\Psi_a]\ [\Psi_b]\ [\Psi_c]\,\big],\ [\Psi_2] := \Big[\,[\widetilde{\Psi}_a]\ [\widetilde{\Psi}_b]\ [\widetilde{\Psi}_c]\,\Big]. \tag{27}$$

Using (25), (26), (27), the complete set of low-order-face-cell-based shape functions on the tetrahedron is written as

$$[\Psi_\nabla] := \big[\,[\Psi_0]\ [\Psi_F]\ [\Psi_I]\,\big]. \tag{28}$$

Let

$$K_{s,\cdot} = \int_{\triangle_s} [\nabla \cdot \Psi_{\nabla \cdot}]^\top [\nabla \cdot \Psi_{\nabla \cdot}] \tag{29}$$

be the element stiffness matrix with respect to the basis (28) and

$$M_{II,s,\cdot} = \int_{\triangle_s} [\Psi_I^\cdot]^\top \cdot [\Psi_I^\cdot] \tag{30}$$

be the block of the interior bubbles of the mass matrix. The following orthogonality results can be shown.

Theorem 6.1 *Let the set* $[\Psi_{\nabla \cdot}]$ *of basis functions be defined in* (28)*. Then, the fluxes* $[\nabla \cdot \Psi_I^\cdot]$ *are* L_2*-orthogonal to* $[\nabla \cdot \Psi_{\nabla \cdot}]$*. Moreover, the stiffness matrix* $K_{s,\cdot}$ (29) *is diagonal up to the* 4×4 *low-order block* $a_{\mathrm{div}}([\Psi_0],[\Psi_0])$*.*
The number of nonzero matrix entries per row in the matrix $M_{II,s,\cdot}$ (30) *is bounded by a constant independent of the polynomial degree* p*.*

Proof. The first result can be proved by straightforward computation. For the mass matrix, the assertion follows by evaluation of the matrix entries using the algorithm described in section 8, see also [16].

Due to a construction based on the Jacobi type polynomials (14), the nonzero pattern of the matrix $M_{II,s,\cdot}$ in (30) has again a stencil like structure as the matrices M_{II,s,∇_3} and K_{II,s,∇_3} in (21), (22) for the H^1 case. Also the growth of the condition number is as $\mathcal{O}(p^4)$. However, the absolute numbers for a fixed polynomial degree p are higher than for the H^1 case.
The divergence of the inner basis functions vanishes for the first part and coincides with the higher-order L_2-optimal Dubiner basis functions for the second part. Hence, the results for the element stiffness matrix $K_{s,\cdot}$ are strongly related to the L_2 results of Section 4. Namely, $K_{s,\cdot}$ is diagonal up to the low-order block. The nonzero pattern for mass and stiffness matrix is displayed in Figure 5 for $p = 15$.
Besides sparsity the appropriately chosen weights imply a tremendous improvement in condition numbers of the system matrices (even for curved element geometries) as reported in [16].

7 Sparsity optimized $H(\mathbf{curl})$-conforming basis functions

The sparsity results for $H(\mathrm{curl})$-conforming basis functions included in this section will be presented in a forthcoming paper [17]. Again, the general construction principle follows [54] and [62]. The sparsity optimization will be performed only for the interior basis functions. Hence, in the sequel we restrict ourselves only to the definition of interior functions, while the edge and face based functions can be taken from [54].
The interior (cell-based) basis functions are constructed in two types. First we define the curl-free shape functions by the gradients

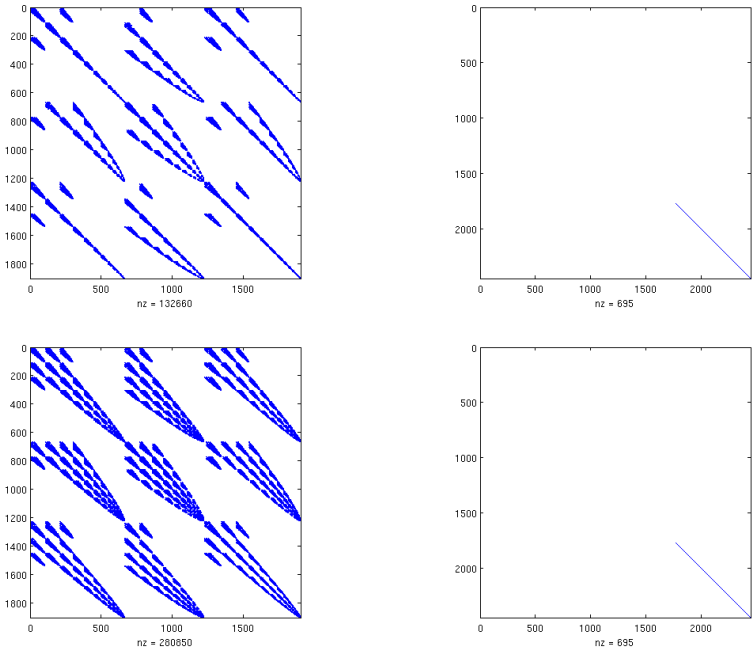

Fig. 5 Optimally weighted Jacobi-type basis $[\Psi_{\nabla\cdot}]$ for $p = 15$: Above: Sparsity pattern of inner block $\widehat{M}_{II,\cdot}$ of element mass (left, above) and element stiffness matrix $\widehat{K}_{\cdot}$ (right, above) on reference tetrahedron $\hat{\triangle}$. Below: Sparsity pattern of inner block $M_{II,s,\cdot}$ of mass matrix (left, below) and stiffness matrix $K_{s,\cdot}$ on a general affine tetrahedron $\triangle_s$ (right, below).

$$\begin{aligned} \varphi_{ijk}^{(b)}(x,y,z) &:= \nabla\big(u_i(x,y,z)\, v_{ij}(x,y,z)\, w_{ijk}(x,y,z)\big), \\ & i \geq 2; j,k \geq 1; i+j+k \leq p+1 \end{aligned} \tag{31}$$

and complete the basis with the non-curl free cell-based shape functions

$$\begin{aligned} \tilde{\varphi}_{1jk}^{(a)}(x,y,z) &:= \varphi_1^{[1,2]}(x,y,z) v_{1j}(x,y,z) w_{1jk}(x,y,z), \\ & j,k \geq 1;\ j+k \leq p-1, \\ \tilde{\varphi}_{ijk}^{(b)}(x,y,z) &:= \nabla u_i(x,y,z) v_{ij}(x,y,z) w_{ijk}(x,y,z), \\ & i \geq 2; j,k \geq 1; i+j+k \leq p+1, \\ \tilde{\varphi}_{ijk}^{(c)}(x,y,z) &:= \nabla\left(u_i(x,y,z) v_{ij}(x,y,z)\right) w_{ijk}(x,y,z), \\ & i \geq 2; j,k \geq 1; i+j+k \leq p+1, \end{aligned} \tag{32}$$

where $\varphi_1^{[1,2]}$ is the Nédélec function (15), and u_i, v_{ij} and w_{ijk} are defined in (14). Finally, we denote the row vectors of the corresponding basis functions as

- $[\Phi_b] = \left[\phi^{(b)}_{ijk}(x,y,z)\right]_{i\geq 2,j,k,\geq 1}^{i+j+k\leq p+1}$ as the gradient fields, and
- $[\widetilde{\Phi}_a] = \left[\widetilde{\phi}^{(a)}_{1jk}(z)\right]_{j,k=1}^{j+k\leq p-1}$,
- $[\widetilde{\Phi}_b] = \left[\widetilde{\phi}^{(b)}_{ijk}(x,y,z)\right]_{i\geq 2,j,k,\geq 1}^{i+j+k\leq p+1}$ and
- $[\widetilde{\Phi}_c] = \left[\widetilde{\phi}^{(c)}_{ijk}(x,y,z)\right]_{i\geq 2,j,k,\geq 1}^{i+j+k\leq p+1}$

as the non curl free functions. The set of interior basis functions is denoted by

$$[\Psi_I^{\times}] := \left[\,[\Phi_b]\;[\Phi_2]\,\right] \;\text{ with }\quad [\Phi_2] := \left[\,[\widetilde{\Phi}_a]\;[\widetilde{\Phi}_b]\;[\widetilde{\Phi}_c]\,\right]. \tag{33}$$

Finally, we introduce

$$K_{s,II,\times} = \int_{\triangle_s} [\nabla\times\Psi_{\nabla\times}]^{\top}\cdot[\nabla\times\Psi_{\nabla\times}] \;\text{ and }\; M_{s,II,\times} = \int_{\triangle_s} [\Psi_{\nabla\times}]^{\top}\cdot[\Psi_{\nabla\times}] \tag{34}$$

as the stiffness and mass matrix with respect to the interior bubbles (33), respectively.

Theorem 7.1 *The matrices $K_{s,II,\times}$ and $M_{s,II,\times}$* (34) *are sparse matrices having a bounded number of nonzero entries per row. The total number of nonzero entries grows as $\mathcal{O}(p^3)$.*

Proof. The result follows from the construction principle of the basis functions in (31), (32) and Theorems 5.3 and 6.1. We refer the reader for a more detailed discussion to [17].

8 Integration by rewriting

In this section we present the algorithm that is used to evaluate the matrix entries for different spaces and choices of basis functions. As indicated earlier, the basic idea is to apply a rewriting procedure to the given integrands that yields a reformulation of the integrand as a linear combination of products of the form

$$\left(\frac{1-x}{2}\right)^{\alpha} p_i^{\alpha}(x)\,p_j^{\alpha}(x).$$

These terms then can be evaluated directly by the Jacobi orthogonality relation (4). Below we use the short-hand notation $w_\alpha(x) = \left(\frac{1-x}{2}\right)^{\alpha}$ for the weight function.
For the necessary rewriting steps several relations between Jacobi polynomials and integrated polynomials are needed that have been proven in [19, 14, 15] and are summarized in the next lemma.

Lemma 8.1 *Let $p_n^\alpha(x)$ and $\hat{p}_n^\alpha(x)$ be the polynomials defined in* (3) *and* (5)*. Then for all $n \geq 1$ we have the relations*

$$\hat{p}_n^\alpha(x) = \frac{2(n+\alpha)}{(2n+\alpha-1)(2n+\alpha)} p_n^\alpha(x) + \frac{2\alpha}{(2n+\alpha-2)(2n+\alpha)} p_{n-1}^\alpha(x) - \frac{2(n-1)}{(2n+\alpha-1)(2n+\alpha-2)} p_{n-2}^\alpha(x), \qquad \alpha \geq -1, \quad (35)$$

$$\hat{p}_n^\alpha(x) = \frac{2}{2n+\alpha-1}[p_n^{\alpha-1}(x) + p_{n-1}^{\alpha-1}(x)], \qquad \alpha > -1, \quad (36)$$

$$(\alpha-1)\hat{p}_n^\alpha(x) = (1-x)\, p_{n-1}^\alpha(x) + 2\, p_n^{\alpha-2}(x), \qquad \alpha > 1. \quad (37)$$

$$p_n^{\alpha-1} = \frac{1}{2n+\alpha}[(n+\alpha)p_n^\alpha(x) - n\, p_{n-1}^\alpha(x)], \qquad \alpha > -1, \quad (38)$$

After decoupling the integrands by means of the Duffy transformation, the integrals are evaluated in the order given by the dependencies of the parameters α. For each of these univariate integrals the following algorithm is executed:

1. Collect integrands depending on the current integration variable,
2. For each integrand: Rewrite integrated Jacobi polynomials in terms of Jacobi polynomials using (35), (36), or (37),
3. Collect integrands depending on the current integration variable,
4. For each integrand: Adjust Jacobi polynomials to appearing weight functions,
5. Collect integrands depending on the current integration variable,
6. For each integrand: Evaluate integrals using orthogonality relation (4).

The two steps of the algorithm that need further explanations are steps 2 and 4. Indeed, let us consider steps 2 and 4 in detail: which of the identities relating integrated Jacobi polynomials and Jacobi polynomials (35)- (37) have to be used in step 2 depends on the difference $\gamma-\alpha$ of the parameters of $\hat{p}_n^\alpha(\zeta)$ and of the weight function $w_\gamma(\zeta)$.

2. Rewrite $w_\gamma(\zeta)\hat{p}_n^\alpha(\zeta)$ in terms of Jacobi polynomials
   (a) $\gamma-\alpha \geq 0$: transform integrated Jacobi polynomials to Jacobi polynomials with same parameter using (35).
   (b) $\gamma-\alpha = -1$: transform integrated Jacobi polynomials to Jacobi polynomials with parameter $\alpha-1$ using (36).
   (c) $\gamma-\alpha = -2$: use the mixed relation (37) to obtain

$$w_\gamma(\zeta)\hat{p}_n^{\gamma+2}(\zeta) = \frac{2}{\gamma+1}\left(w_\gamma(\zeta)p_n^\gamma(\zeta) + w_{\gamma+1}(\zeta)p_{n-1}^{\gamma+2}(\zeta)\right).$$

If none of the cases 2(a)-2(c) applies, the algorithms interrupts and returns the unevaluated integrand for further examination. Such an output can lead either to a readjustment of the parameters of the basis functions, or to the discovery of a new relation between Jacobi polynomials that needs to be added to the given rewrite

rules. This finding of new, necessary identities can again be achieved with the assistance of symbolic computation, e.g., by means of Koutschan's package HolonomicFunctions [45] or Kauers' package SumCracker [43].
Rewriting the Jacobi polynomials $p_n^\alpha(\zeta)$ in terms of $p_n^\gamma(\zeta)$ fitting to the appearing weights $w_\gamma(\zeta)$ in step 4, means lifting the polynomial parameter α using (38) $(\gamma-\alpha)$ times. This transformation is performed recursively for each appearing Jacobi polynomial.

4. Rewrite the Jacobi polynomials $p_n^\alpha(\zeta)$ in terms of Jacobi polynomials fitting to the appearing weights $w_\gamma(\zeta)$ $(\gamma-\alpha>0)$ by lifting the polynomial parameter α using (38) $(\gamma-\alpha)$-times, i.e., written in explicit form we have

$$p_n^\alpha(\zeta)=\sum_{m=0}^{\gamma-\alpha}(-1)^k\begin{pmatrix}\gamma-\alpha\\ m\end{pmatrix}\frac{(n+\gamma-m)^{\underline{\gamma-\alpha-m}}n^{\underline{m}}}{(2n+\gamma-m+1)^{\underline{\gamma-\alpha+1}}}(2n-2m+\gamma+1)p_{n-m}^\gamma(\zeta),$$

where $a^{\underline{k}}=a(a-1)\cdot\ldots\cdot(a-k+1)$ denotes the falling factorial.

If $\gamma-\alpha<0$ the algorithm interrupts. In this step of the algorithm polynomials down to degree $n-\gamma+\alpha$ are introduced. Hence this transformation is a costly one as it increases the number of terms significantly.

Acknowledgement:

This work has been supported by the FWF-projects P20121-N12 and P20162-N18, the Austrian Academy of Sciences, the Spezialforschungsbereich "Numerical and Symbolic Scientific Computing" (SFB F013) , the doctoral program "Computational Mathematics" (W1214) and the FWF Start Project Y-192 on "3D hp-Finite Elements: Fast Solvers and Adaptivity".

References

1. M. Abramowitz and I. Stegun, editors. *Handbook of mathematical functions*. Dover-Publications, 1965.
2. M. Ainsworth. A preconditioner based on domain decomposition for *h-p* finite element approximation on quasi-uniform meshes. *SIAM J. Numer. Anal.*, 33(4):1358–1376, 1996.
3. M. Ainsworth and J. Coyle. Hierarchic finite element bases on unstructured tetrahedral meshes. *Int. J. Num. Meth. Eng.*, 58(14):2103–2130, 2003.
4. M. Ainsworth and L. Demkowicz. Explicit polynomial preserving trace liftings on a triangle. *Math. Nachr.*, 282(5):640–658, 2009.
5. M. Ainsworth and B. Guo. An additive Schwarz preconditioner for *p*-version boundary element approximation of the hypersingular operator in three dimensions. *Numer. Math.*, 85(3):343–366, 2000.
6. P. Appell. Sur des polynômes de deux variables analogues aux polynômes de jacobi. *Arch. Math. Phys.*, 66:238–245, 1881.
7. I. Babuška and B. Q. Guo. The *h-p* version of the finite element method for domains with curved boundaries. *SIAM J. Numer. Anal.*, 25(4):837–861, 1988.

8. I. Babuška, A. Craig, J. Mandel, and J. Pitkäranta. Efficent preconditioning for the p-version finite element method in two dimensions. *SIAM J.Numer.Anal.*, 28(3):624–661, 1991.
9. I. Babuška, M. Griebel, and J. Pitkäranta. The problem of selecting the shape functions for a p-type finite element. *Int. Journ. Num. Meth. Eng.*, 28:1891–1908, 1989.
10. C. Bernardi, M. Dauge, and Y. Maday. Polynomials in weighted Sobolev spaces: Basics and trace liftings. Technical Report R 92039, Universite Pierre et Marie Curie, Paris, 1993.
11. Ch. Bernardi, M. Dauge, and Y. Maday. The lifting of polynomial traces revisited. *Math. Comp.*, 79(269):47–69, 2010.
12. S. Beuchler. Multi-grid solver for the inner problem in domain decomposition methods for p-FEM. *SIAM J. Numer. Anal.*, 40(3):928–944, 2002.
13. S. Beuchler. Wavelet solvers for hp-FEM discretizations in 3D using hexahedral elements. *Comput. Methods Appl. Mech. Engrg.*, 198(13-14):1138–1148, 2009.
14. S. Beuchler and V. Pillwein. Shape functions for tetrahedral p-fem using integrated Jacobi polynomials. *Computing*, 80:345–375, 2007.
15. S. Beuchler and V. Pillwein. Completions to sparse shape functions for triangular and tetrahedral p-fem. In U. Langer, M. Discacciati, D.E. Keyes, O.B. Widlund, and W. Zulehner, editors, *Domain Decomposition Methods in Science and Engineering XVII*, volume 60 of *Lecture Notes in Computational Science and Engineering*, pages 435–442, Heidelberg, 2008. Springer. Proceedings of the 17th International Conference on Domain Decomposition Methods held at St. Wolfgang / Strobl, Austria, July 3–7, 2006.
16. S. Beuchler, V. Pillwein, and S. Zaglmayr. Sparsity optimized high order finite element functions for H(div) on simplices. Technical Report 2010-04, DK Computational Mathematics, JKU Linz, 2010.
17. S. Beuchler, V. Pillwein, and S. Zaglmayr. Sparsity optimized high order finite element functions for $H(curl)$ on tetrahedral meshes. Technical Report Report RICAM, Johann Radon Institute for Computational and Applied Mathematics, Linz, 2011. in preparation.
18. S. Beuchler, R. Schneider, and C. Schwab. Multiresolution weighted norm equivalences and applications. *Numer. Math.*, 98(1):67–97, 2004.
19. S. Beuchler and J. Schöberl. New shape functions for triangular p-fem using integrated jacobi polynomials. *Numer. Math.*, 103:339–366, 2006.
20. A. Bossavit. *Computational Electromagnetism: Variational formulation, complementary, edge elements*. Academic Press Series in Electromagnetism. Academic Press Inc., 1989.
21. D. Braess. *Finite Elemente*. Springer. Berlin-Göttingen-Heidelberg, 1991.
22. D. Braess. Approximation on simplices and orthogonal polynomials. In *Trends and applications in constructive approximation*, volume 151 of *Internat. Ser. Numer. Math.*, pages 53–60. Birkhäuser, Basel, 2005.
23. F. Chyzak. Gröbner bases, symbolic summation and symbolic integration. In *Gröbner bases and applications (Linz, 1998)*, volume 251 of *London Math. Soc. Lecture Note Ser.*, pages 32–60. Cambridge Univ. Press, Cambridge, 1998.
24. F. Chyzak. An extension of Zeilberger's fast algorithm to general holonomic functions. *Discrete Math.*, 217(1-3):115–134, 2000. Formal power series and algebraic combinatorics (Vienna, 1997).
25. F. Chyzak and B. Salvy. Non-commutative elimination in Ore algebras proves multivariate identities. *J. Symbolic Comput.*, 26(2):187–227, 1998.
26. P. Ciarlet. *The Finite Element Method for Elliptic Problems*. North–Holland, Amsterdam, 1978.
27. M. Costabel, M. Dauge, and L. Demkowicz. Polynomial extension operators for H^1, $H(\mathrm{curl})$ and $H(\mathrm{div})$-spaces on a cube. *Math. Comp.*, 77(264):1967–1999, 2008.
28. L. Demkowicz. *Computing with hp Finite Elements*. CRC Press, Taylor and Francis, 2006.
29. L. Demkowicz, J. Gopalakrishnan, and J. Schöberl. Polynomial extension operators. I. *SIAM J. Numer. Anal.*, 46(6):3006–3031, 2008.
30. L. Demkowicz, J. Gopalakrishnan, and J. Schöberl. Polynomial extension operators. II. *SIAM J. Numer. Anal.*, 47(5):3293–3324, 2009.

31. L. Demkowicz, J. Kurtz, D. Pardo, M. Paszyński, W. Rachowicz, and A. Zdunek. *Computing with hp-adaptive finite elements. Vol. 2*. Chapman & Hall/CRC Applied Mathematics and Nonlinear Science Series. Chapman & Hall/CRC, Boca Raton, FL, 2008. Frontiers: three dimensional elliptic and Maxwell problems with applications.
32. L. Demkowicz, P. Monk, L. Vardapetyan, and W. Rachowicz. De Rham diagram for hp finite element spaces. *Computers and Mathematics with Aplications*, 39(7-8):29–38, 2000.
33. M. O. Deville and E. H. Mund. Finite element preconditioning for pseudospectral solutions of elliptic problems. *SIAM J. Sci. Stat. Comp.*, 18(2):311–342, 1990.
34. M. Dubiner. Spectral methods on triangles and other domains. *J. Sci. Computing*, 6:345, 1991.
35. C.F. Dunkl and Y. Xu. *Orthogonal polynomials of several variables*, volume 81 of *Encyclopedia of Mathematics and its Applications*. Cambridge University Press, Cambridge, 2001.
36. T. Eibner and J. M. Melenk. An adaptive strategy for hp-FEM based on testing for analyticity. *Comput. Mech.*, 39(5):575–595, 2007.
37. A. George. Nested dissection of a regular finite element mesh. *SIAM J. Numer. Anal.*, 10:345–363, 1973.
38. B. Guo and W. Cao. An iterative and parallel solver based on domain decomposition for the hp- version of the finite element method. *J. Comput. Appl. Math.*, 83:71–85, 1997.
39. S. A. Ivanov and V. G. Korneev. On the preconditioning in the domain decomposition technique for the p-version finite element method. Part I. Technical Report SPC 95-35, Technische Universität Chemnitz-Zwickau, December 1995.
40. S. A. Ivanov and V. G. Korneev. On the preconditioning in the domain decomposition technique for the p-version finite element method. Part II. Technical Report SPC 95-36, Technische Universität Chemnitz-Zwickau, December 1995.
41. S. Jensen and V. G. Korneev. On domain decomposition preconditioning in the hierarchical $p-$version of the finite element method. *Comput. Methods. Appl. Mech. Eng.*, 150(1–4):215–238, 1997.
42. G.M. Karniadakis and S.J.Sherwin. *Spectral/HP Element Methods for CFD*. Oxford University Press. Oxford, 1999.
43. M. Kauers. SumCracker – A Package for Manipulating Symbolic Sums and Related Objects. *Journal of Symbolic Computation*, 41(9):1039–1057, 2006.
44. V. Korneev, U. Langer, and L. Xanthis. On fast domain decomposition methods solving procedures for hp-discretizations of 3d elliptic problems. *Computational Methods in Applied Mathematics*, 3(4):536–559, 2003.
45. C. Koutschan. HolonomicFunctions (User's Guide). Technical Report 10-01, RISC Report Series, University of Linz, Austria, January 2010.
46. J. M. Melenk, C. Pechstein, J. Schöberl, and S. Zaglmayr. Additive Schwarz preconditioning for p-version triangular and tetrahedral finite elements. *IMA J. Num. Anal.*, 28:1–24, 2008. to appear.
47. J.M. Melenk, K. Gerdes, and C. Schwab. Fully discrete hp-finite elements: Fast quadrature. *Comp. Meth. Appl. Mech. Eng.*, 190:4339–4364, 1999.
48. P. Monk. *Finite Element Methods for Maxwell's Equations*. Numerical Mathematics and Scientific Computation. The Clarendon Press Oxford University Press, New York, 2003.
49. R. Munoz-Sola. Polynomial liftings on a tetrahedron and applications to the h-p version of the finite element method in three dimensions. *SIAM J. Numer. Anal.*, 34(1):282–314, 1996.
50. J.C. Nédélec. Mixed finite elements in $\mathbb{R}^3$. *Numerische Mathematik*, 35(35):315–341, 1980.
51. L. F. Pavarino. Additive schwarz methods for the p-version finite element method. *Numer. Math.*, 66(4):493–515, 1994.
52. M. Petkovšek, H.S. Wilf, and D. Zeilberger. $A = B$. A K Peters Ltd., Wellesley, MA, 1996.
53. A. Quateroni and A. Valli. *Numerical Approximation of partial differential equations*. Number 23 in Springer Series in Computational Mathematics. Springer. Berlin-Heidelberg-New York, 1997.
54. J. Schöberl and S. Zaglmayr. High order Nédélec elements with local complete sequence properties. *International Journal for Computation and Mathematics in Electrical and Electronic Engineering (COMPEL)*, 24:374–384, 2005.

55. J. Schöberl and S. Zaglmayr. hp finite element De Rham sequences on hybrid meshes, in preperation.
56. C. Schwab. *p− and hp−finite element methods. Theory and applications in solid and fluid mechanics.* Clarendon Press. Oxford, 1998.
57. S. J. Sherwin and G. E. Karniadakis. A new triangular and tetrahedral basis for high-order finite element methods. *Int. J. Num. Meth. Eng.*, 38:3775–3802, 1995.
58. P. Solin, K. Segeth, and I. Dolezel. *Higher-Order Finite Element Methods*. Chapman and Hall, CRC Press, 2003.
59. G. Szegö. *Orthogonal Polynomials*. AMS Colloquium Publications, Volume XXIII. 3 edition, 1974.
60. F.G. Tricomi. *Vorlesungen über Orthogonalreihen*. Springer. Berlin-Göttingen-Heidelberg, 1955.
61. H.S. Wilf and D. Zeilberger. An algorithmic proof theory for hypergeometric (ordinary and "q") multisum/integral identities. *Invent. Math.*, 108(3):575–633, 1992.
62. S. Zaglmayr. *High Order Finite Elements for Electromagnetic Field Computation*. PhD thesis, Johannes Kepler University, Linz, Austria, 2006.
63. D. Zeilberger. A fast algorithm for proving terminating hypergeometric identities. *Discrete. Math.*, 80:207–211, 1990.
64. D. Zeilberger. A holonomic systems approach to special functions identities. *J. Comput. Appl. Math.*, 32(3):321–368, 1990.
65. D. Zeilberger. The method of creative telescoping. *J. Symbolic Computation*, 11:195–204, 1991.